



澳門科技大学
MACAU UNIVERSITY OF SCIENCE AND TECHNOLOGY

Kelvin-Helmholtz Instability and Its Applications on the Space Environment of Earth and Mars

– Group Meeting of the Planetary Space Physics

WANG,XING

State Key Laboratory of Lunar and Planetary Sciences, Space Science Institute,
Macau University of Science and Technology



Oct.16, 2020. Macau, China



Outline

Introduction of Kelvin-Helmholtz Instability

Basic Concept of Kelvin-Helmholtz Instability

Natural Phenomena of Kelvin-Helmholtz Instability

Magnetohydrodynamics(MHD) Kelvin-Helmholtz Instability

Applications on the Space Environment of Earth and Mars

Earth

Mars

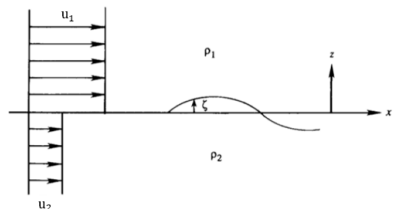
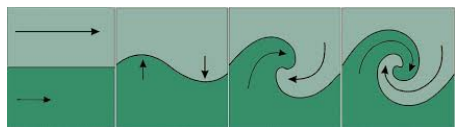
Further Works About Study of KHI on the Martian Space Environment



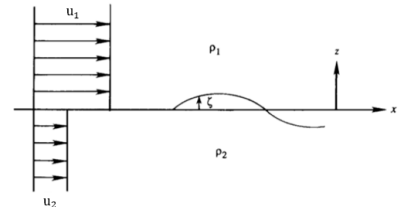
Basic Concept of Kelvin-Helmholtz Instability

- Kelvin-Helmholtz instability (KHI) was first studied by Hermann von Helmholtz in 1868 and by William Thomson (Lord Kelvin) in 1871;
- incompressible and inviscid fluids;
- relative and irrotational motion;
- the velocity u and density ρ profiles are uniform in each fluid layer;
- u and ρ are discontinuous at the interface: shear flow;
- The condition of instability:

$$(u_1 - u_2)^2 > \frac{g(\rho_2^2 - \rho_1^2)}{k\rho_1\rho_2}$$



- at the top: lighter fluid ρ_1 with u_1 ;
- at the bottom: heavier fluid ρ_2 with u_2 ;
- vertical and horizontal domains are infinite;
- surface tension, molecular viscosity and density diffusion are ignored.
- Incompressible fluid: $\nabla \cdot \mathbf{v} = 0$; Potential flow: $\mathbf{v} = \nabla \phi$; then: $\nabla^2 \phi = 0$;
- For each fluid, $\phi_i = u_i x + \phi'_i, i = 1, 2$; then



$$\nabla^2 \phi'_i = 0 \quad (1)$$

- and conditions:

$$\phi'_1 \rightarrow 0 \quad z \rightarrow \infty, \quad \phi'_2 \rightarrow 0 \quad z \rightarrow -H$$

$$\frac{\partial \phi_i}{\partial z} \Big|_{z=\zeta} \approx \frac{\partial \phi_i}{\partial z} \Big|_{z=0}, \quad \frac{\partial \phi'_i}{\partial z} = \frac{\partial \zeta}{\partial t} + u_i \frac{\partial \zeta}{\partial x} \quad \text{at} \quad z = 0 \quad (2)$$



- For inviscid fluid, the Navier-Stokes equation is:

$$\rho \frac{\partial \mathbf{v}}{\partial t} + \rho (\mathbf{v} \cdot \nabla) \mathbf{v} = -\nabla p + \rho \mathbf{g}$$

- Considering the flow is irrotational, then:

$$(\mathbf{v} \cdot \nabla) \mathbf{v} = \frac{1}{2} \nabla v^2 - \mathbf{v} \times (\nabla \times \mathbf{v}) = \frac{1}{2} \nabla v^2$$

- Then we can get:

$$\rho_i \frac{\partial \nabla \phi_i}{\partial t} + \nabla \left(\frac{1}{2} \rho_i (\nabla \phi_i)^2 + \rho_i g z \right) = -\nabla p_i$$

- Substituting $\phi_i = u_i x + \phi'_i$ into above equation, and considering $p_1 = p_2$, we can obtain:

$$\rho_1 \left[\frac{\partial \phi'_1}{\partial t} + u_1 \frac{\partial \phi'_1}{\partial x} + g \zeta \right]_{z=0} = \rho_2 \left[\frac{\partial \phi'_2}{\partial t} + u_2 \frac{\partial \phi'_2}{\partial x} + g \zeta \right]_{z=0} \quad (3)$$



- Assuming the perturbation terms are the following forms:

$$(\zeta, \phi'_1, \phi'_2) = (\hat{\zeta}, \hat{\phi}'_1, \hat{\phi}'_2) e^{ik(x-ct)}$$

- According the Laplace equation $\nabla^2 \phi'_i = 0$, we can find the solutions:

$$\hat{\phi}'_1 = A e^{-kz}, \hat{\phi}'_2 = B e^{kz}$$

- Substituting the above solutions into Eq(2) and Eq(3), we can get $Dx = 0$, where $x = [A, B, \hat{\zeta}]^T$, and

$$D = \begin{pmatrix} ik\rho_1(u_1 - c) & ik\rho_2(-u_2 + c) & g(\rho_1 - \rho_2) \\ 1 & 0 & i(u_1 - c) \\ 0 & 1 & i(-u_2 + c) \end{pmatrix}$$

- We can get a non-trivial solution when:

$$|D| = c^2(\rho_1 + \rho_2) - 2c(u_1\rho_2 + u_2\rho_1) + \frac{g}{k}(\rho_1 - \rho_2) + (u_1^2\rho_1 + u_2^2\rho_2) = 0$$



- This is a quadratic equation and the solution for c are:

$$c = \frac{u_1\rho_2 + u_2\rho_2}{\rho_1 + \rho_2} \pm \sqrt{\frac{(u_1\rho_2 + u_2\rho_2)^2}{(\rho_1 + \rho_2)^2} - \frac{\frac{g}{k}(\rho_1 - \rho_2) + (u_1^2\rho_1 + u_2^2\rho_2)}{\rho_1 + \rho_2}}$$

- If the result under square root is negative, c is a complex number:
 $c = c_r + ic_i$ and $c_i > 0$; the solutions are unstable:

$$(\zeta, \phi'_1, \phi'_2) = \left(\hat{\zeta}, \hat{\phi}'_1, \hat{\phi}'_2 \right) e^{ik(x-ct)} = \left(\hat{\zeta}, \hat{\phi}'_1, \hat{\phi}'_2 \right) e^{ik(x-c_r t)} e^{kc_i t}$$

- At this condition:

$$\frac{(u_1\rho_2 + u_2\rho_2)^2}{(\rho_1 + \rho_2)^2} < \frac{\frac{g}{k}(\rho_1 - \rho_2) + (u_1^2\rho_1 + u_2^2\rho_2)}{\rho_1 + \rho_2}$$

- After rearrangement of terms, we arrive at:

$$(u_1 - u_2)^2 > \frac{g(\rho_2^2 - \rho_1^2)}{k\rho_1\rho_2}$$



Natural Phenomena of KHI: Arts



Hiroshige Utagawa "Vortices in the Konaruto stream"



Vincent Van Gogh "La Nuit Etoilee"



Natural Phenomena of KHI: Ocean and Cloud

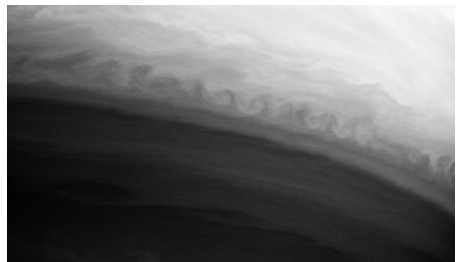




Natural Phenomena of KHI: Giant Planets



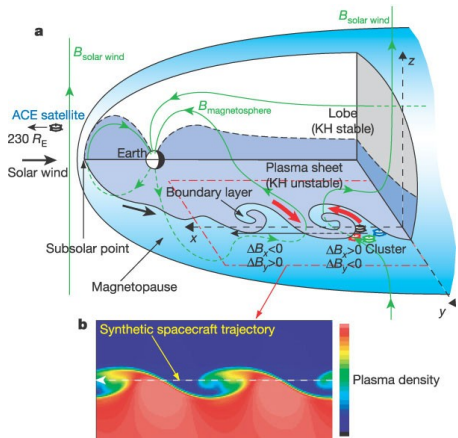
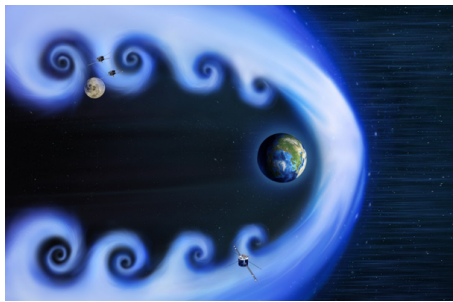
Jupiter, great spot, Voyager 2(NASA)



Saturn pictured by Cassini(NASA)



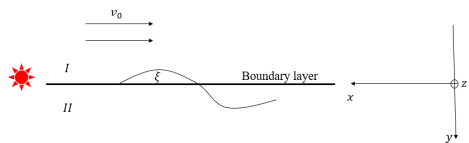
Natural Phenomena of KHI: Space Plasma



Hasegawa et al. 2004

Mathematical Model of MHD KHI

- Considering a hydromagnetic perturbation near a boundary of discontinuous flow velocity;
- Assuming incompressible ideal MHD perturbations;



- Linearized MHD equations:

$$\nabla \cdot \mathbf{v} = 0$$

$$m_i n \frac{d\mathbf{v}}{dt} = \mathbf{J} \times \mathbf{B} - \nabla p$$

$$\mathbf{E} + \mathbf{v} \times \mathbf{B} = \eta \mathbf{J}$$

$$\nabla \times \mathbf{B} = \mu_0 \mathbf{J}$$

$$\frac{\partial \xi}{\partial t} = \mathbf{v}_1$$

$$m_i n_0 \ddot{\xi} = \frac{1}{\mu_0} [(\nabla \times \mathbf{B}_1) \times \mathbf{B}_0 + (\nabla \times \mathbf{B}_0) \times \mathbf{B}_1] - \nabla p_1$$

$$\mathbf{B}_1 = \nabla \times (\xi \times \mathbf{B}_0) = (\mathbf{B}_0 \cdot \nabla) \xi - (\xi \cdot \nabla) \mathbf{B}_0 - \mathbf{B}_0 (\nabla \cdot \xi)$$



■ Considering $\nabla \cdot \mathbf{B}_1 = \nabla \cdot \mathbf{B}_0 = 0$ and $\nabla \cdot \mathbf{v}_1 = \nabla \cdot \boldsymbol{\xi} = 0$, we can get:

$$\nabla^2 \tilde{p}_1 = \frac{1}{\mu_0} \nabla \cdot [(\mathbf{B}_0 \cdot \nabla) \mathbf{B}_1 + (\mathbf{B}_1 \cdot \nabla) \mathbf{B}_0] - \nabla \cdot (m_i n_0 \ddot{\boldsymbol{\xi}}) = 0$$

where \tilde{p}_1 is the total pressure given by $\tilde{p}_1 = \frac{\mathbf{B}_1 \cdot \mathbf{B}_0}{\mu_0} + p_1$;

■ This is a Laplace equation, the wave-like solution is given by:

$$\tilde{p}_1 = p_0 e^{-\kappa|y|} e^{i(k_x x + k_z z - \omega t)}, \quad \kappa = \sqrt{k_x^2 + k_z^2}$$

■ Substituting the above solution into the linearized MHD equations, we can get:

$$[\mu_0 m_i n_0 \omega^2 - (\mathbf{k} \cdot \mathbf{B}_0)^2] \boldsymbol{\xi} = \mu_0 \nabla \tilde{p}_1 + \mathbf{c}$$

where

$$\mathbf{c} = (\mathbf{B}_0 \cdot \nabla)[(\boldsymbol{\xi} \cdot \nabla) \mathbf{B}_0 + \mathbf{B}_0 (\nabla \cdot \boldsymbol{\xi})] - (\mathbf{B}_1 \cdot \nabla) \mathbf{B}_0$$

vanishes in a uniform plasma. In that case:

$$\boldsymbol{\xi} = \frac{\nabla \tilde{p}_1}{m_i n_0 [\omega^2 - (\mathbf{k} \cdot \mathbf{v}_A)^2]}$$

where $\mathbf{v}_A = \frac{\mathbf{B}_0}{\sqrt{\mu_0 m_i n_0}}$ is Alfvén velocity, and $\mathbf{k} = k_x \mathbf{e}_x + k_z \mathbf{e}_z$.



- I: $y < 0$; II: $y > 0$;
- ω_I is Doppler shifted with respect to ω_{II} : $\omega_I = \omega - \mathbf{k} \cdot \mathbf{v}_0$, $\omega_{II} = \omega$;
- Total pressure \tilde{p}_1 is continuous at the boundary;
- We can get the dispersion relation:

$$\frac{1}{n_{0I}[(\omega - \mathbf{k} \cdot \mathbf{v}_0)^2 - (\mathbf{k} \cdot \mathbf{v}_A)_I^2]} + \frac{1}{n_{0II}[\omega^2 - (\mathbf{k} \cdot \mathbf{v}_A)_{II}^2]} = 0$$

Or:

$$(n_{0I} + n_{0II})\omega^2 - 2n_{0I}(\mathbf{k} \cdot \mathbf{v}_0)\omega + n_{0I}[(\mathbf{k} \cdot \mathbf{v}_0)^2 - (\mathbf{k} \cdot \mathbf{v}_A)_I^2] - n_{0II}(\mathbf{k} \cdot \mathbf{v}_A)_{II}^2 = 0$$

- The solution for ω are:

$$\omega = \frac{1}{n_{0I} + n_{0II}} \left[n_{0I}(\mathbf{k} \cdot \mathbf{v}_0) \pm \sqrt{\Delta} \right]$$

- ω will be a complex number $\omega = \omega_r + i\omega_i$ when:

$$\Delta = \left(\frac{1}{n_{0I}} + \frac{1}{n_{0II}} \right) [n_{0I}(\mathbf{k} \cdot \mathbf{v}_A)_I^2 + n_{0II}(\mathbf{k} \cdot \mathbf{v}_A)_{II}^2] - (\mathbf{k} \cdot \mathbf{v}_0)^2 < 0$$

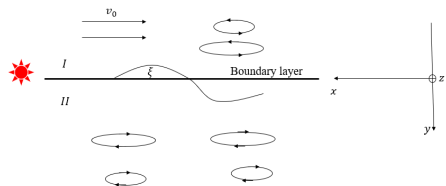
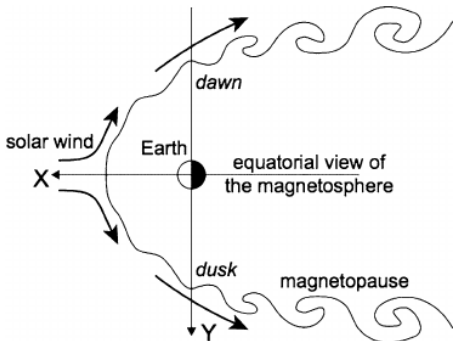


The condition of KHI:

$$(\mathbf{k} \cdot \mathbf{v}_0)^2 > \left(\frac{1}{n_{0I}} + \frac{1}{n_{0II}} \right) [n_{0I}(\mathbf{k} \cdot \mathbf{v}_A)_I^2 + n_{0II}(\mathbf{k} \cdot \mathbf{v}_A)_{II}^2]$$

KHI occurs more easily when: $(\mathbf{k} = k_x \mathbf{e}_x + k_z \mathbf{e}_z)$

$$\mathbf{k} \perp \mathbf{B}_0 \quad or \quad \mathbf{k} \parallel \mathbf{v}_0$$





KHI on the Earth's magnetosphere

Why study KHI

- **How the solar wind plasma, momentum and energy enter into the Earth's magnetosphere?**
- Several scenarios of plasma transport: magnetic reconnection, diffusive particle transport via turbulence, anomalous transport due the conversion of KH surface waves to kinetic Alfvén waves;
- **Southward IMF:**
 1. Magnetic reconnection occur at the subsolar magnetopause;
 2. Leading to storage of magnetic energy and reconnection in the magnetotail;
- **Northward IMF:**
 1. Magnetic reconnection occur mostly at tailward of the cusps;
 2. Solar wind plasma penetration is observed at the Low Latitude Boundary Layer(LLBL) and in the central plasma sheet;
 3. Other physical phenomena have been proposed: high-latitude reconnection and the KHI.



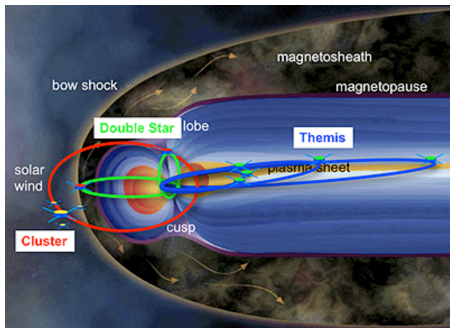
Questions

- Does KHI lead to the development of rolled-up vortices along the magnetopause?
- Are they rare or a common feature?
- Is there a dawn–dusk asymmetry? if yes what causes it?
- Does the KHI only occurs during Northward IMF and near the LLBL(the Low Latitude Boundary Layer)?
- What are the physical mechanisms within a KHI vortex allowing magnetosheath plasma to enter or magnetospheric plasma to exit the magnetosphere?
- How does this phenomenon develop from birth to collapse along the magnetopause?
- How is magnetic reconnection initiated within KH rolled-up vortices?
- What is the contribution of the KHI vs. magnetic reconnection in terms of plasma entry?

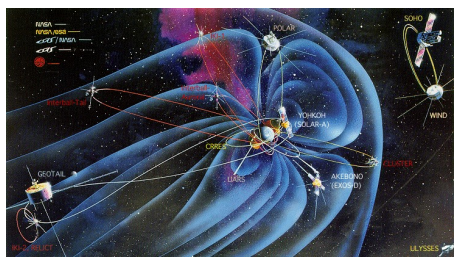


KHI on the Earth's magnetosphere

Earth's Magnetospheric Missions:

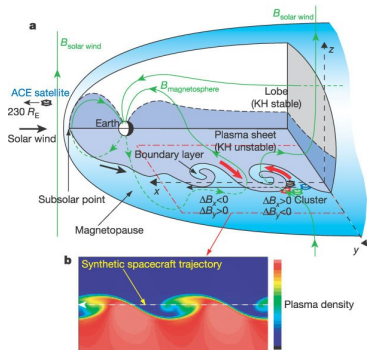


Orbit of Cluster, THEMIS and Double Star

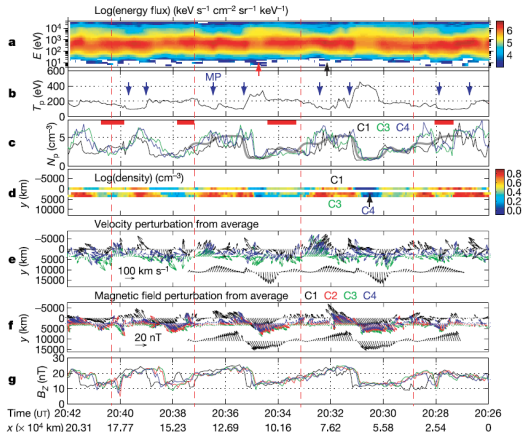


Orbit of Geotail mission

- **THEMIS:** The Time History of Events and Macroscale Interactions during Substorms.



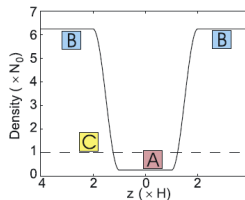
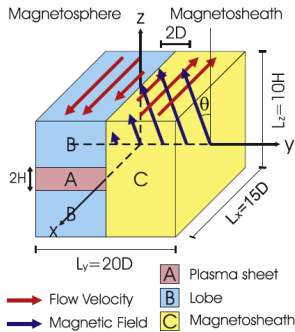
Hasegawa et al. 2004



Hasegawa et al. 2004

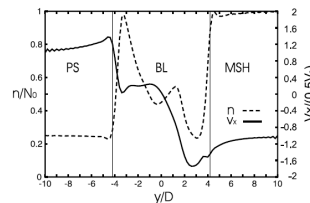
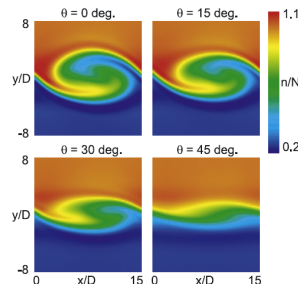
- 20 November 2001, northward IMF;
- KH waves can roll-up and evolve into $4 - 5.5 \times 10^4 \text{ km}$ wide vortices.

■ Tenuous plasma must rotate faster than a denser plasma:



Takagi et al. 2006

WANG,XING • Group Meeting-Kelvin-Helmholtz Instability •



Takagi et al. 2006



These vortices are not rare under northward IMF conditions:

Table 1. KHI Events Observed by THB and THC From 2008 to 2009

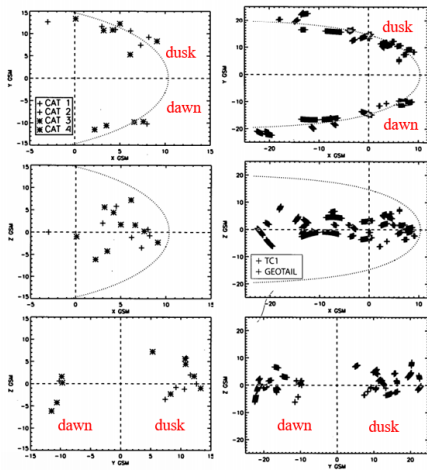
Probe	Date (yyyy-mm-dd)	Time Interval (hhmm-hhmm)	GSM Position (R_E)	T_{KH} (s)	V_{ph} (km/s)	λ_{KH} (R_E)	IMF (nT)	CA (degree)	V_{SW} (km/s)
THC	2008-4-13	0240-0440	(-5.1, 17.2, 1.6)	325	111	5.7	(-0.1, 3.0, 2.1)	50	577
THC	2008-5-1	1150-1240	(-4.5, 18.5, -2.3)	242	170	6.5	(-3.6, 1.8, 2.1)	39	469
THB	2008-5-15	1430-1510	(-4.2, 16.9, 1.2)	115	174	3.1	(5.5, -2.2, 1.4)	-55	331
THB	2008-9-13	1212-1237	(4.8, -11.6, 0.1)	95	141	2.1	(1.6, 1.0, 2.1)	25	313
THC	2008-9-17	1205-1240	(7.9, -10.4, 1.1)	147	117	2.7	(2.2, -1.0, 4.5)	-12	431
THB	2008-9-17	1310-1400	(5.4, -13.1, 0.1)	119	177	3.3	(2.7, -0.9, 4.6)	-10	430
THC	2008-11-6 ^a	0852-0952	(-0.3, -15.3, 4.6)	134	156	3.3	(2.1, -0.9, 1.5)	-31	288
THC	2008-11-18	0720-0800	(-2.3, -17.0, 3.4)	174	129	3.5	(-1.0, -1.0, 3.1)	-17	348
THB	2009-4-6	0710-0835	(-19.4, 25.0, 3.3)	448	203	14.3	(0.7, 1.8, 2.2)	39	405
THC	2009-5-29	0000-0040	(4.5, 14.9, 1.9)	258	120	4.9	(-1.3, -1.3, 0.6)	-67	404
THC	2009-6-6	0023-0113	(6.5, 12.6, 0.4)	95	152	2.3	(-0.8, -3.2, 2.8)	-48	327
THB	2009-10-3	0740-0820	(0.9, -16.0, 4.5)	204	168	5.4	(-0.6, 0.2, 2.0)	6	325
THB	2009-10-12	0200-0245	(10.6, 5.2, 1.7)	354	77	4.3	(-1.0, -3.1, 2.6)	-47	416
THB	2009-11-2	1850-1950	(-9.8, -19.9, -1.0)	212	248	8.3	(2.8, -3.1, 2.0)	-58	349

Table 2. Instruments Providing the Magnetic Field and Plasma Measurements and Counts of the KH Wave Events for Each Spacecraft^a

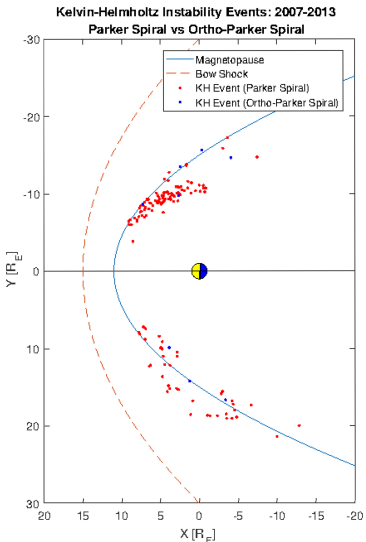
Spacecrafts	Magnetic Field	Plasma	Count
Geotail	Magnetic Field Experiment (MGF) [Kokubun et al., 1994]	Low Energy Particle Experiment (LEP) [Mukai et al., 1994]	20
TC – 1	Flux Gate Magnetometer (FGM) [Carr et al., 2005]	Hot Ion Analyzer (HIA) [Rème et al., 2005]	17
Cluster	Flux Gate Magnetometer (FGM) [Balogh et al., 2001]	Cluster Ion Spectrometry (CIS) [Rème et al., 2001]	5
THEMIS	FluxGate Magnetometer (FGM) [Auster et al., 2008]	ElectroStatic Analyzer (ESA) [McFadden et al., 2008]	14



Possible dawn-dusk asymmetry:

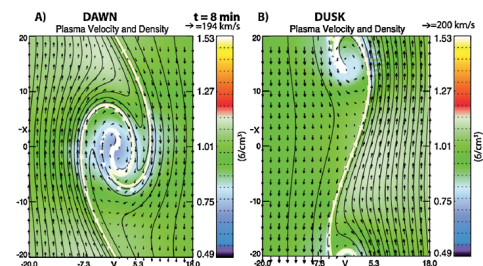
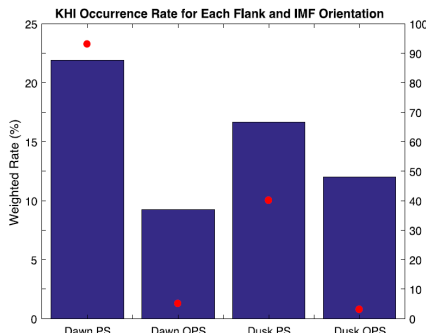


Taylor et al. 2012



Henry et al. 2017

- Asymmetric heating: temperature at the dawnside plasma sheet denser and hotter 30 – 40% than duskside (Hasegawa et al. 2003; Wing et al. 2005);



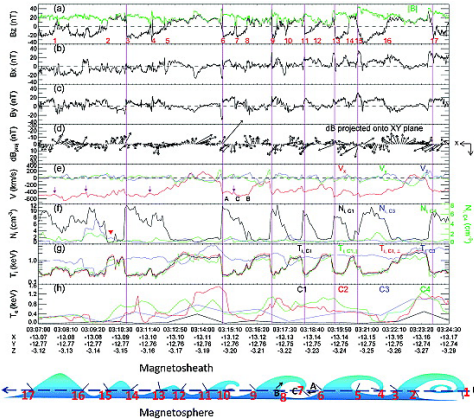
Masson and Nykyri 2018

Masson and Nykyri 2018

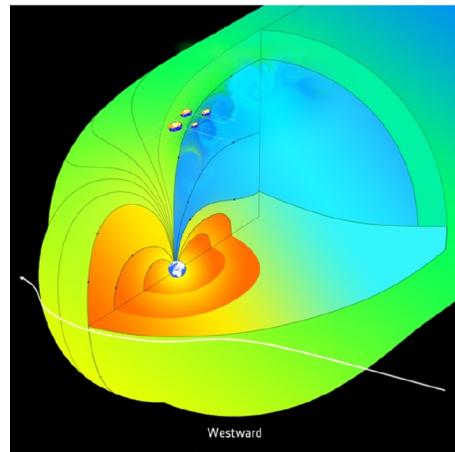
- The dawn-favoured asymmetry of the KH waves and ion scale waves may therefore explain the origin of the observed plasma sheet temperature and density asymmetry.



■ Southward IMF and downward IMF conditions:

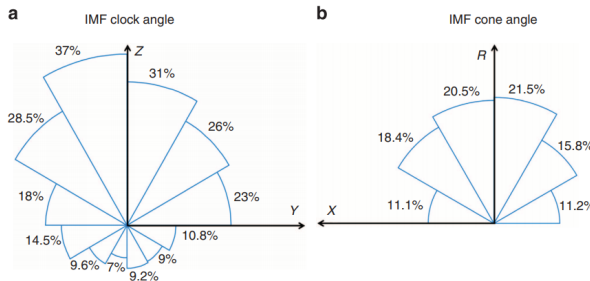


Hwang et al. 2011



Masson and Nykyri 2018

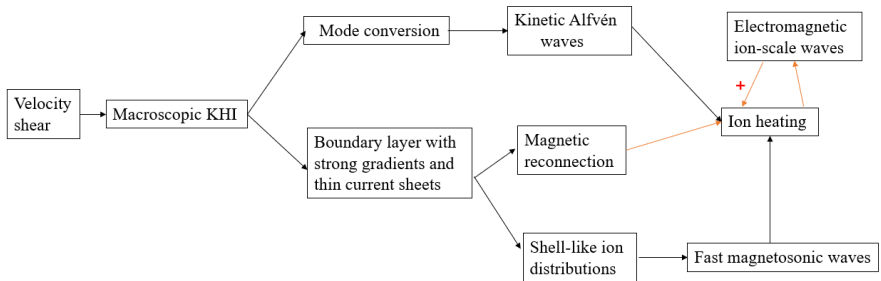
- When velocity shear and magnetic shear are not aligned, the KH modes and tearing modes are unstable;
- the KHI onset condition can be satisfied more often for northward than for southward IMF conditions.



Kavosi and Raeder 2015

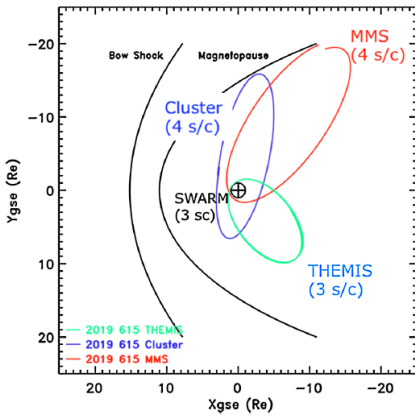
- clock angle= $\arctan \frac{B_y}{B_z}$, cone angle= $\arccos \frac{B_x}{B}$, $R = \sqrt{Y^2 + Z^2}$;
- Samples: 7 years, THEMIS crossed magnetopause during 960h, northward IMF: 500h, southward IMF: 460h;
- the KHI: 35% for northward IMF, 20% for equatorial plane IMF, 10% for southward IMF.

- Several possible cross-scale energy transport mechanisms associated with the KHI:



Masson and Nykyri 2018

■ Cluster, MMS, THEMIS and Swarm orbits in June 2019:

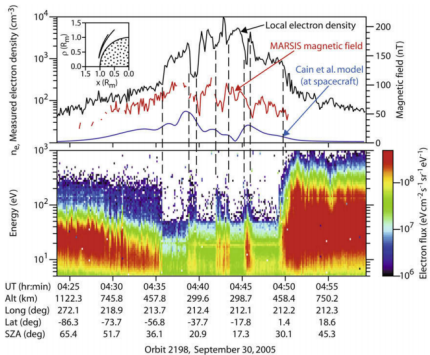


Masson and Nykyri 2018

- These new and unique observations will enable to tackle the following open questions:
- 1. What is the evolution of a Kelvin–Helmholtz vortex from birth to collapse?
- 2. How is magnetic reconnection initiated within K–H rolled-up vortices?
- 3. Do they enable solar wind plasma to enter into magnetospheres?
- 4. What is their role in the formation and existence of the cold dense plasma sheet?

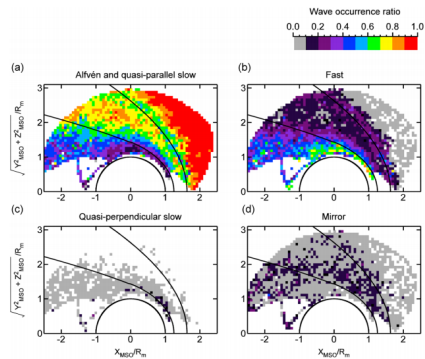
KHI on the Martian Space Environment

- Several observations made at Mars are suggestive of the KHI operating at its ionosphere:



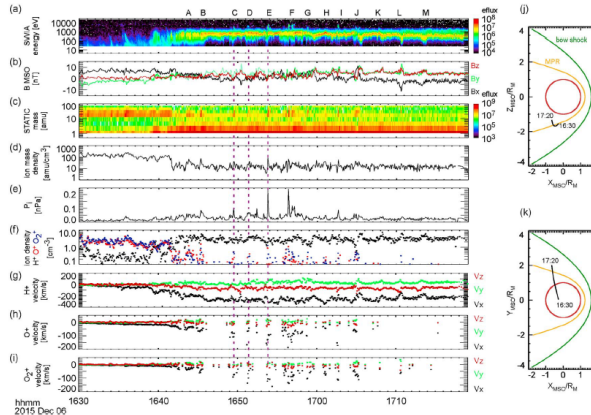
Gurnett et al. 2010(Mars Express)

WANG,XING • Group Meeting-Kelvin-Helmholtz Instability •



Ruhunusiri, Halekas, Connerney, et al.
2015(MAVEN)

- Periodic perturbations: energy($T \sim 3\text{min}$, (a)A-M); magnetic field(b);
- Heavy ions(O^+ , O_2^+ ,(c)), $\rho \uparrow$ (d); $p_i \uparrow$ (e);



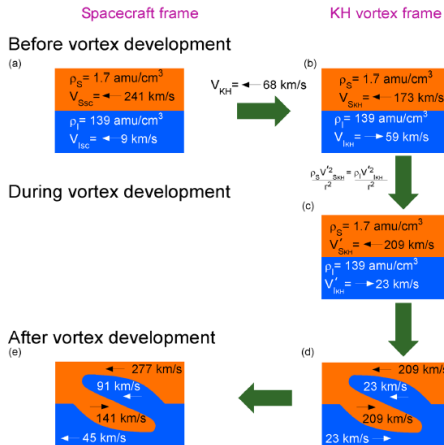
Ruhunusiri, Halekas, McFadden, et al. 2016

- At boundary: ρ, v_x of $\text{H}^+ \downarrow$ and periodic(g), ρ, v_x of O^+ , $\text{O}_2^+ \uparrow$ (f,h,i).



■ Rolled up vortices: $v_{magnetosphere} > v_{sheath}$, Earth ✓, Mars ×;

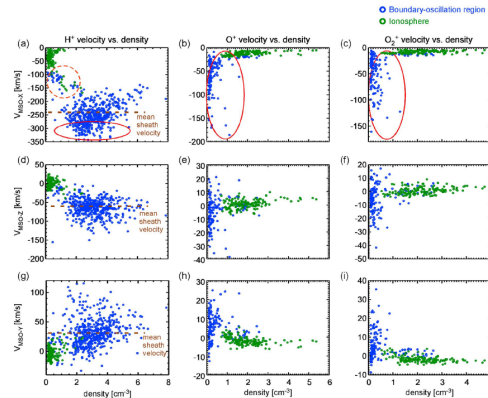
KH vortex development at Mars



Ruhunusiri, Halekas, McFadden, et al. 2016

$$\blacksquare \quad \rho_S \frac{v_{SKH}^2}{r^2} = \rho_I \frac{v_{IKH}^2}{r^2}; \quad v_{KH} = \frac{1}{2} \left(\frac{v_S + v_I}{2} + \frac{\rho_S v_S + \rho_I v_I}{\rho_S + \rho_I} \right).$$

WANG,XING • Group Meeting-Kelvin-Helmholtz Instability



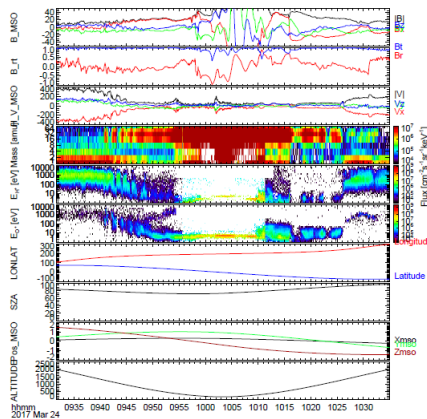
- Fully developed vortex:
 1. $v_{xs} \uparrow < 0$, and $> v_{xs0}$;
 2. $v_{xi} \uparrow < 0$, and $> v_{xi0}$;
 3. $v_{xs} \downarrow > 0$;
 4. $v_{xi} \downarrow < 0$, and $> v_{xi0}$;
- (a): $v_{H^+} < 0$ and $> v_{ms}$, 1, 4✓;
- (b), (c): $v_{O^+}, v_{O_2^+} < 0$ and $> v$ in ionosphere, 2✓;
- (a): v_{H^+} in the boundary oscillation < 0 , and $< v_{ms}$, 3×.
- Not fully rolled up!

Ruhunusiri, Halekas, McFadden, et al. 2016

- The growth rate of KHI: $\gamma_{max} = 8 \times 10^{-3} s^{-1}$, the spatial growth rate corresponding to the temporal growth rate: $k_i = \frac{\gamma}{V_g} = 1.2 \times 10^{-4} \text{ km}^{-1}$;
- Amplitude of KH vortex: $A = A_0 e^{k_i \delta d}$; $\delta d = 9100 \text{ km}$, if fully rolled up, $A = 3A_0$; but $\frac{A}{A_0} < 3$ according to Penz et al. 2004.

Further Works

- Finding the KH waves on the Martian ionopause based on MAVEN data;
- Estimating the ion escape rate caused by KHI.



- the ion escape rate: $f \approx \frac{n_i n_c}{T_M}$;
- n_c is the plasma cloud number,
 $T_M \approx 120 - 240s$;

Table 1
Loss of atomic oxygen from Mars by different escape processes

Process	Loss of oxygen (s^{-1})	Authors
Atmospheric sputtering	4.3×10^{23}	Leblanc and Johnson (2002)
Photochemical processes	5×10^{24}	Lammer and Bauer (1991)
Average ion pick up	3×10^{24}	Lammer et al. (2003a)
Plasma clouds maximum	3×10^{24}	this work
Plasma clouds minimum	2×10^{23}	this work

Penz et al. 2004



参考文献 I

-  DA Gurnett et al. "Large density fluctuations in the Martian ionosphere as observed by the Mars Express radar sounder". In: *Icarus* 206.1 (2010), pp. 83–94.
-  H Hasegawa et al. "Transport of solar wind into Earth's magnetosphere through rolled-up Kelvin–Helmholtz vortices". In: *Nature* 430.7001 (2004), pp. 755–758.
-  Zachary W Henry et al. "On the dawn-dusk asymmetry of the Kelvin-Helmholtz instability between 2007 and 2013". In: *Journal of Geophysical Research: Space Physics* 122.12 (2017), pp. 11–888.
-  K-J Hwang et al. "Kelvin-Helmholtz waves under southward interplanetary magnetic field". In: *Journal of Geophysical Research: Space Physics* 116.A8 (2011).



参考文献 II

-  Shiva Kavosi and Joachim Raeder. "Ubiquity of Kelvin–Helmholtz waves at Earth's magnetopause". In: *Nature Communications* 6 (2015), p. 7019.
-  Dong Lin et al. "Properties of Kelvin-Helmholtz waves at the magnetopause under northward interplanetary magnetic field: Statistical study". In: *Journal of Geophysical Research: Space Physics* 119.9 (2014), pp. 7485–7494.
-  A Masson and K Nykyri. "Kelvin–Helmholtz instability: Lessons learned and ways forward". In: *Space Science Reviews* 214.4 (2018), p. 71.
-  T Penz et al. "Ion loss on Mars caused by the Kelvin–Helmholtz instability". In: *Planetary and Space Science* 52.13 (2004), pp. 1157–1167.



參考文献 III

-  Suranga Ruhunusiri, JS Halekas, JEP Connerney, et al. “Low-frequency waves in the Martian magnetosphere and their response to upstream solar wind driving conditions”. In: *Geophysical Research Letters* 42.21 (2015), pp. 8917–8924.
-  Suranga Ruhunusiri, JS Halekas, JP McFadden, et al. “MAVEN observations of partially developed Kelvin-Helmholtz vortices at Mars”. In: *Geophysical Research Letters* 43.10 (2016), pp. 4763–4773.
-  K Takagi et al. “Kelvin-Helmholtz instability in a magnetotail flank-like geometry: Three-dimensional MHD simulations”. In: *Journal of Geophysical Research: Space Physics* 111.A8 (2006).
-  MGGT Taylor et al. “Spatial distribution of rolled up Kelvin-Helmholtz vortices at Earth’s dayside and flank magnetopause”. In: *Annales Geophysicae*. Vol. 30. 6. 2012, pp. 1025–1035.



谢谢！